

IARA: An Orchestrating Improved Artificial Raindrop Algorithm for VNFs Deployment in Network Function Virtualization

Hejun Xuan, Xuelin Zhao, Zhenghui Liu and Yanling Li

Abstract—Network Function Virtualization (NFV) can provide the resource according to the request and can improve the flexibility of the network. It has become the key technology of 5G communication. Resource scheduling for virtual network function service chain (VNF-SC) is the key issue of the NFV. In this paper, the problem of routing and VNFs deployment for VNF service chain (VNF-SC) in inter-data center elastic optical networks (inter-DC EONs) is investigated. We investigate the inter-DC EONs that each data center only can provide some specific VNFs, and the system resources of all the data centers are limited. In addition, part of required VNFs in each VNF-SC is dependent, i.e., the relative order of required VNFs is fixed. To solve the challenging problem, we first establish a mix-integer programming model. Then, to make the population distributed on the search domain uniformly, uniform design method was developed. In addition, an improved artificial raindrop algorithm (IARA) for the established model, which inspired by particle swarm optimization and differential evolution, is proposed to solve the maximum model efficiently. Finally, to demonstrate high performance of the designed algorithm, a series of experiments are conducted in several different experimental scenes. Experimental results indicate that the proposed algorithm can obtain the better results than compared algorithm.

Index Terms—VNF-SC, EONs, VNFs deployment, uniform design, artificial raindrop algorithm

I. INTRODUCTION

NETWORK function virtualization (NFV) becomes a hot research field as it can facilitate the flexibility of the network services[1], [2]. Optical network virtualization has many advantages and can help virtual networks with different topologies.[3], [4], [5], [6]. What is more, it enables network operators to operate different virtual optical networks that share a common physical network, simplifies optical layer resource management, provides flexible spectrum assignment scheme, and offers secure application services[7], [8], [9].

In this work, we investigate the problem of spectrum assignment for VNF service chain (VNF-SC) in inter-data center elastic optical networks. Different from the previous

works, we investigate the inter-data center elastic optical networks that each data center only can provide some specific VNFs, and the system resources of all the data centers are limited. In addition, part of required VNFs in each VNF-SC is dependent, i.e., the relative order of required VNFs is fixed. What is more, we not only consider to minimize the maximum index of used frequency slots and the occupied system resource but also to minimize the cost of generating these spectra. The major contributions of this study are summarized as follows:

- We investigate the inter-data center elastic optical networks that each data center only can provide some specific VNFs, and the system resources of all the data centers are limited.
- We divide the VNFs in each VNF-SC into two parts, i.e., parts of required VNFs are independent, and the others are dependent.
- To make the population distributed on the search domain uniformly, uniform design method was developed. Based on this, an improved artificial raindrop algorithm(IARA) for the established model, which inspired by particle swarm optimization and differential evolution, is proposed to solve the maximum model efficiently.

The rest of this paper is organized as follows. Some related works are introduced in sectionII. Section III gives the network architecture and the optimization model. To solve the optimization model effectively, we propose a improve artificial raindrop algorithm in section IV. To evaluate the algorithm proposed, simulation experiments are conducted, and the experimental results are analyzed in Section V. The paper is concluded with a summary in Section VI.

II. RELATED WORKS

In general, VNF-SC has many advantages, such as high bandwidth capacity and low power consumption [10], [11], [12], [13]. So, VNF-SC is especially beneficial for inter-data center networks. However, some challenges will be faced. In recent years, the widely investigate problem are VNF-SC routing and VNFs deployment [14], [15], [16], [17], [18], [19]. To optimize the cost of the VNFs deployment and multi-cast routing and spectrum assignment jointly for orchestrating multi-cast NFV trees in an inter-data center elastic optical networks, mixed integer linear programming model is established, and three heuristic algorithms are proposed[10]. To minimize the total cost of the energy consumption and the revenue loss due to QoS degradation, an efficient algorithm, which is based on the back-to-back strategy, is designed[14]. For the sake of solving VNF-SC

Manuscript received April 14, 2020; revised July 09, 2020. This work is supported by National Natural Science Foundation of China (No.61572391, 61572417, 31900710), Science and Technology Department of Henan Province (No.182102210132, 182102210537), Innovation Team Support Plan of University Science and Technology of Henan Province (No.19IRTSTHN014), Nanhu Scholars Program for Young Scholars of XYNUN, Youth Sustentation Fund of Xinyang Normal University (No.2019-QN-040), University Students Sustentation Fund of Xinyang Normal University (No.2019-DXS-035).

Hejun Xuan, Xuelin Zhao, Zhenghui Liu and Yanling Li are with the school of Computer and Information Technology, Xinyang Normal University, Henan Xinyang, China, 464000 e-mail: xuanhejun0896@126.com.

Zhenghui Liu and Yanling Li is with Henan Key Lab. of Analysis and Application of Education Big Data, Xinyang Normal University, Henan Xinyang, China, 464000.

and resource allocation problem, Wang, et al.[16] formulated a mixed-integer linear programming model and proposed a heuristic-based algorithm, which is divided into two sub-algorithms: one-hop optimal traffic scheduling problem and VNF chain composition problem. To respect user's requirements and maximize provider revenue, Marouen, et al. [20] proposed a novel approach based on eigendecomposition for the VNFs deployment in elastic optical networks and cloud environments. Considering elastic optical networking and DC capacity constraints, an effective algorithm based noncooperative mixed-strategy gaming approach is proposed[21]. The relatively long setup latency and complicated network control and management caused by on-demand virtual network function service chain (vNF-SC) provisioning in inter-data center elastic optical networks was addressed[22]. A provisioning framework with resource pre-deployment to resolve the aforementioned challenge has been developed. Literature [23] provided a model of the adaptive and dynamic VNF allocation problem considering also VNF migration, and formulated the optimization problem as an integer linear programming (ILP) and provide a heuristic algorithm for allocating multiple VNF-FGs. Literature [24] proposed an incentive-driven virtual network function VNF-SC framework for optimizing the cross-stratum resource provisioning in multi-broker orchestrated inter-data center elastic optical networks (IDC-EONs). The proposed framework employs a non-cooperative hierarchical game-theoretic mechanism, where the resource brokers and the VNF-SC users play the leader and the follower games, respectively. A novel resource allocation architecture which enables energy-aware SFC for SDN-based networks, considering also constraints on delay, link utilization, server utilization is proposed[25]. In addition, a set of heuristic to find near-optimal solutions in timescales suitable for practical applications are designed.

III. PROBLEM FORMATION

A. Network and VNF-SC Description

We use a directed graph $G(V, E)$ to denote an inter-data center elastic optical networks (EON), where $V = \{v_1, v_2, \dots, v_{N_V}\}$ represents the set of the nodes in the network with N_V being the number of nodes and v_i is the i -th optical node, respectively. For the node v_i , we can describe it as $v_i = \{DC_i, IT_i\}$, where DC_i is the data center, which is connected to node v_i , and IT_i is the system resource on the data center. In our work, we assume that each data center only can apply some specific virtual network functions (VNFs), and we denote the set of VNFs as $VNF_i^V = \{VNF_{i_1}, VNF_{i_2}, \dots, VNF_{i_d}, \dots, VNF_{i_{N_{vnf}^i}}\}$, where N_{vnf}^i is the number of VNFs that data center DC_i can provide, and $VNF_{i_d} \in VNF$, where VNF is a set that includes all the VNFs and can be denoted by $VNF = \{VNF_1, VNF_2, \dots, VNF_{N_{vnf}}\}$ with N_{vnf} being the number of VNFs. If no data center is connected to the node v_i , we have $DC_i = \emptyset$ and $IT_i = \emptyset$. N_{dc} denote the number of data centers. $E = \{l_{ij} | v_i, v_j \in V\}$ represents the set of optical links with l_{ij} being the link between node v_i and node v_j , and N_E is the number of links in the inter-data center EONs. $F = \{f_1, f_2, \dots, f_{N_F}\}$ represents the set of available frequency slots in each link, where N_F is the number of available frequency slots.

$R = \{r_1, r_2, \dots, r_m, \dots, r_{N_R}\}$ denotes a set of VNF-SCs, where N_R is the number of VNF-SC, and r_k is the k -th VNF-SC. For $\forall r_k \in R$, we denote r_k as $r_k = (s_k, d_k, b_k, VNF_k^R, SeqVNF_k^R, c_k)$, where s_k, d_k and b_k are the source node, destination node and primarily required frequency slots, respectively. $VNF_k^R = \{VNF_{k_1}, \dots, VNF_{k_a}, \dots, VNF_{k_{N_k^R}}\}$ and $SeqVNF_k^R = \{seqVNF_{k_1}, \dots, seqVNF_{k_b}, \dots, seqVNF_{k_{sN_k^R}}\}$ are two sets of VNFs that r_k required, and N_k^R and sN_k^R are the number of VNFs in VNF_k^R and $SeqVNF_k^R$, respectively. In VNF_k^R , all the required VNFs are independent, and the order of these VNFs is flexible. However, all the required VNFs in $SeqVNF_k^R$ are dependent, that is to say, they must be arranged in a special order. $c_k = \{c_k^1, c_k^2, \dots, c_k^{N_k^R + sN_k^R}\}$ is the set of required frequency slots after the realization of homologous VNFs.

B. Mathematical Modeling

The problem of routing, VNFs deployment and spectrum assignment for inter-Data center elastic optical networks should complete the following tasks: First, proper paths should be selected for each VNF-SC, i.e., routing. Then, required VNFs of VNF-SC should be deployed in the proper data centers. Finally, spectrum assignment scheme should be determined for each VNF-SCs. Thus, we can establish an optimization model in the following for this challenging problem.

1) *Objective function*: The objective is to minimize the cost of two terms to serve all the VNF-SCs. The objective function is expressed by

$$\min H = \min \left\{ \alpha_1 \frac{N_{max}^{used}}{N_F} + \alpha_2 \frac{\sum r_k \mu B_k}{N_F N_E} + \alpha_3 \frac{\sum v_i IT_i^{used}}{\sum v_i IT_i} \right\} \quad (1)$$

where α and β are two factors introduced to adjust the importance of the three terms, and we have $0 \leq \alpha_1, \alpha_2, \alpha_3 \leq 1$, $\alpha_1 + \alpha_2 + \alpha_3 = 1$. μ is the cost to generate one frequency slot. N_{max}^{used} is the maximum index of used frequency slots, and B_k is the number of frequency slots of r_k required on all links.

2) *Constraints*: Some constraints should be satisfied for the model as follows:

Constraint (a): Each VNF-SC $r_k (\forall r_k \in R)$ must occupy one and only one path. That is,

$$\sum_{q=1}^{N_{Q_k}} \lambda_k^q = 1, \forall r_k \in R \quad (2)$$

where $Q_k = \{Q_k^1, Q_k^2, \dots, Q_k^{N_{Q_k}}\}$ is the set of candidate paths for the VNF-SC r_k with N_{Q_k} being the number of candidate paths. λ_k^q is a boolean variable, $\lambda_k^q = 1$ if and only if the path Q_k^q is occupied by r_k , otherwise, $\lambda_k^q = 0$.

Constraint (b): All the data centers, which are connected to the nodes of each candidate paths in Q_k , can provide all the VNFs of r_k required. This constraint can be given by

$$(VNF_k^R \cup SeqVNF_k^R) \subseteq \bigcup_{v_i \in V_k^q} VNF_i^V, \forall Q_k^q \in Q_k \quad (3)$$

where V_k^q denotes the sets of data centers in path Q_k^q .

Constraint (c): VNFs on the data centers, which are connected to the nodes of each candidate paths in Q_k , can satisfy the specific order of the VNFs in $SeqVNF_k^R$. That is

$$seqVNF_a \in \bigcup_{v_i \in V_k^q(b)} VNF_i^V, \forall \langle seqVNF_a, seqVNF_b \rangle \quad (4)$$

where $\langle seqVNF_a, seqVNF_b \rangle$ represents that $seqVNF_a$ should be implemented before $seqVNF_b$. $V_k^q(b)$ denotes the sets of data centers in path Q_k^q , and these data centers must be located in front of the data center that $seqVNF_b$ is deployed in.

Constraint (d): Each VNF of $r_k (\forall r_k \in R)$ required only can be deployed in one data center. We can express this constraint by

$$\sum_{v_i \in V_k^q} \psi_{kt}^i = 1, \forall VNF_t \in (VNF_k^R \cup SeqVNF_k^R) \quad (5)$$

where ψ_{kt}^i is a boolean variable, $\psi_{kt}^i = 1$ if and only if the VNF_t or $seqVNF_t$ of r_k is deployed in DC_i , otherwise, $\psi_{kt}^i = 0$.

Constraint (e): The number of VNFs deployed in each data center should not be exceed its capacity, we have

$$\sum_k \sum_t \psi_{kt}^i \leq IT_i, \forall v_i \in V \quad (6)$$

Constraint (f): For $r_k (\forall r_k \in R)$, the start frequency slot on different links of a path must be identical. This can be given by

$$f_{l_{ij}}^k = f_{l_{i'j'}}^k, \forall r_k \in R \quad (7)$$

where $f_{l_{ij}}^k$ and $f_{l_{i'j'}}^k$ are the start frequency slots of r_k on links l_{ij} and $l_{i'j'}$, respectively, and l_{ij} and $l_{i'j'}$ are the different links on the path of r_k occupied.

Constraint (g): Consecutive frequency slots to $r_k (\forall r_k \in R)$ should be assigned. This constraint can be expressed as

$$f_{l_{ij}}^k + B_k + GF - 1 \sum_{u=f_{l_{ij}}^k} \phi_{k,l_{ij}}^{q,u} = B_k + GF, \forall r_k \in R \quad (8)$$

where $\phi_{k,l_{ij}}^{q,u}$ is a boolean variable. $\phi_{k,l_{ij}}^{q,u} = 1$ if and only if the u -th frequency slot on link l_{ij} of path Q_k^q is occupied by r_k , otherwise, $\phi_{k,l_{ij}}^{q,u} = 0$. GF is the number of guaranteed frequency slots.

Constraint (h): For any two VNF-SCs r_k and $r_{k'}$ which occupy the same link l_{ij} , if the start frequency slot index of r_k is smaller than that of $r_{k'}$, this case is denoted by $r_k \prec r_{k'}$. Then these two VNF-SCs should satisfy

$$f_{l_{ij}}^k + B_k + GF \leq f_{l_{ij}}^{k'}, \forall r_k \prec r_{k'} \quad (9)$$

Thus, we can give the mix-integer linear programming

(MILP) model as below:

$$\left\{ \begin{array}{l} \min H = \min \left\{ \alpha_1 \frac{N_{max}^{used}}{NF} + \alpha_2 \frac{\sum_k \mu B_k}{NF NE} + \alpha_3 \frac{\sum_{v_i} IT_i^{used}}{\sum_{v_i} IT_i} \right\} \\ s.t. \\ (a) \sum_{q=1}^{N_{Q_k}} \lambda_k^q = 1; \\ (b) (VNF_k^R \cup SeqVNF_k^R) \subseteq \bigcup_{v_i \in V_k^q} VNF_i^V; \\ (c) seqVNF_a \in \bigcup_{v_i \in V_k^q(b)} VNF_i^V; \\ (d) \sum_{v_i \in V_k^q} \psi_{kt}^i = 1; \\ (e) \sum_k \sum_t \psi_{kt}^i \leq IT_i; \\ (f) f_{l_{ij}}^k = f_{l_{i'j'}}^k; \\ (g) \sum_{u=f_{l_{ij}}^k} \phi_{k,l_{ij}}^{q,u} = B_k + GF; \\ (h) f_{l_{ij}}^k + B_k + GF \leq f_{l_{ij}}^{k'}; \end{array} \right. \quad (10)$$

To solve this mix-integer linear programming model, we propose an effective improved artificial raindrop algorithm (IARA) in section IV.

IV. OVERVIEW OF ARTIFICIAL RAINDROP ALGORITHM AND IMPROVED ARTIFICIAL RAINDROP ALGORITHM

A. Overview of Artificial Raindrop Algorithm

Artificial raindrop algorithm (ARA) derives by the observation of natural rainfall process and simulates the the changing process of a raindrop. The core idea is to follow the raindrops to where they are found occupying the lowest energy state with the largest number-the raindrop pool. In ARA, raindrops are considered as objects and their performance is assessed by corresponding altitude. The location of the lowest elevation corresponds to the optimal solution. In general, ARA includes six stages: raindrop generation, raindrop descent, raindrop collision, raindrop flowing, raindrop pool updating, vapor updating.

Similar to the most meta-heuristic algorithms, ARA searches the optimal solution with an initial population by randomly generating N_p vapors in a limited search space, and each vapor has a corresponding position defined as $v_i = (v_i^1, v_i^2, \dots, v_i^d, \dots, v_i^D)$ $i = 1, 2, \dots, N_p$, where N_p is the population size, D is the dimension of problem, and v_i^d is the position of the i -th vapor in the d -th dimension.

1) *Raindrop Generation*: In general, raindrop is generated by constantly absorbing ambient water vapor. For the sake of simplicity, it is assumed that the raindrop position is the geometric center of ambient water vapor. Thus, its position can be defined as $RP = (x^1, x^2, \dots, x^d, \dots, x^D)$, where $x^d = \frac{1}{N_p} \sum_{i=1}^{N_p} x_i^d$.

2) *Raindrop Descent*: When the influence of external factors is ignored, the raindrop will drop from the cloud to the ground through free-fall. This implies that one component of raindrop position is changed and the raindrop will move to a new position denoted new raindrop. For the raindrop RP , x^{d_j} be the position of raindrop in the d_j -th dimension, in which $d_j (j = 1, 2, 3, 4)$ is chosen arbitrarily from the set $\{1, 2, \dots, D\}$. Thus, the d -th dimension y^d of new raindrop ($NRP = (y^1, y^2, \dots, y^d, \dots, y^D)$) can be obtained by a

linear combination of x^{d_2} , x^{d_3} and x^{d_4} , and defined as follows:

$$y^d = \begin{cases} x^{d_2} + \gamma(x^{d_3} - x^{d_4}) & d = d_1 \\ x^d & otherwise \end{cases} \quad (11)$$

where γ is a random number in $(-1, 1)$ and $d = 1, 2, \dots, D$.

3) *Raindrop Collision*: The new raindrop will be split into a large number of small raindrops when it strikes the ground. These small raindrops ($SRP_i, (i = 1, 2, \dots, N_s)$) will be flying in all directions. For this reason, SRP_i can be defined as follows:

$$SRP_i = NRP + \text{sign}(\alpha - 0.5) \cdot \lg(\beta) \cdot (NRP - v_i) \quad (12)$$

where k , which randomly selected from the set $1, 2, \dots, N_p$ is a index. α and β are two random numbers, and are distributed in the range $(0, 1)$ uniformly. $\text{sign}(\cdot)$ represents the sign function.

4) *Raindrop Flowing*: Under the action of gravity, these $SRP_i (i = 1, 2, \dots, N_p)$ will flow from high altitude to low altitude direction, and most of them will eventually stop at the locations with lower altitude (i.e. the better solutions). In the process of algorithm evolution, these better solutions can provide additional information about the promising progress direction. As a result, the raindrop pool (**RPO**), which has N_{rpo} raindrops, is designed to track these lower positions found so far during the search, and the updating of **RPO** is made as follows: 1) **RPO** is initiated to be any feasible solution of search space; 2) The optimal solution of current population is added to **RPO** after each iteration; 3) If the size of **RPO** exceeds the threshold given in advance, then some solutions in **RPO** will be randomly deleted in order to keep the size of **RPO** stable and reduce calculation amount.

What is more, the flowing direction of raindrop $dSRP_i$ for $SRP_i (i = 1, 2, \dots, N_p)$ can be constructed based on the linear combination of two vectors $dSRP1_i$ and $dSRP2_i$ as follows:

$$dSRP_i = \tau_1 \cdot \theta_i^1 \cdot dSRP1_i + \tau_2 \cdot \theta_i^2 \cdot dSRP2_i \quad (13)$$

where τ_1 and τ_2 are two step parameters of SPR_i flowing, θ_i^1 and θ_i^2 are generated randomly in the range $(0, 1)$. $dSRP1_i$ and $dSRP2_i$ are two vectors and defined as follows:

$$dSRP1_i = \text{sign}(F(RPO_{k_1}) - F(SRP_i)) \cdot (RPO_{k_1} - SRP_i) \quad (14)$$

$$dSRP2_i = \text{sign}(F(RPO_{k_2}) - F(SRP_i)) \cdot (RPO_{k_2} - SRP_i) \quad (15)$$

where RPO_{k_1} and RPO_{k_2} ($1 \leq k_1 \neq k_2 \leq N_{rpo}$) are any two of candidate solutions in **RPO**. $F(\cdot)$ denotes the fitness function. Thus, the i -th new small raindrop ($NSRP_i$) can be defined as

$$NSRP_i = SRP_i + dSRP_i \quad (16)$$

In general, it is necessary to bring a parameter N_{MF} to control the maximum number of flowing. Thus, these new small raindrops will stay in the locations with a lower elevation or evaporate after several flowing because of the parameter N_{MF} .

5) *Vapor Updating*: To make ARA is convergent, in the vapor updating, the N_p best solutions from new small raindrops and vapors are selected using sorting method as the next vapor population.

B. Improved Artificial Raindrop Algorithm (IARA)

1) *Encoding*: To solve the routing and VNF deployment problem by using artificial raindrop algorithm, we should encode the solutions of routing and VNFs deployed. In this work, different encoding scheme are designed. So, there are two RPOs, including routing RPO and VNFs deployment RPO.

Each raindrop in the routing RPO presents a routing scheme for all the VNF-SC. Assuming that $x = (x_1, x_2, \dots, x_{N_R})$ is an raindrop in routing RPO. $x_k = q$ if and only if r_k occupies q -th path in candidate paths set Q_k of r_k , where $Q_k = \{Q_k^1, Q_k^2, \dots, Q_k^K\}$ and K is the number of the candidate paths for all the VNF-SC.

Similarly, each raindrop in VNFs deployment RPO denotes one VNFs deployment scheme for all the VNF-SCs. We assume that $y = (y_k)_{1 \times N_R}$ is an individual in VNFs deployment population, where $y_k = ((y_{k,1}^{VNF}, \dots, y_{k,N_R}^{VNF}), (y_{k,1}^{SeqVNF}, \dots, y_{k,N_R}^{SeqVNF}))$ represent the VNFs in VNF_k^R and $SeqVNF_k^R$ deployment schemes of r_k , respectively. As shown in Fig.1, it denotes a VNF deployment scheme for a VNF-SC. The first column denotes the scheme of VNF deployment of dependent VNFs for R_1 . Three VNFs are deployed on the V_2, V_2 and V_4 . The second column denotes the scheme of VNF deployment of independent VNFs for R_1 . These two VNFs are deployed on the V_4 and V_5 . Similarly, the third and fourth columns are the scheme of VNF deployment of VNFs for R_2 .

	R_1	R_2	R_3	R_4	
	3	2	2	3	} Scheme of VNF deployment
	2	4	1	1	
	2	5	3	3	
	4	0	0	4	
	0	0	0	0	

Fig. 1. An example of encoding scheme for VNF deployment

2) *Improved Raindrop Flowing*: In the improved algorithm, flowing direction of raindrop $dSRP_i$ of $SRP_i (i = 1, 2, \dots, N_p)$ can be constructed based on the linear combination of three vectors $dSRP1_i$, $dSRP2_i$ and $dSRP3_i$ as follows:

$$dSRP_i = \tau_1 \cdot \theta_i^1 \cdot dSRP1_i + \tau_2 \cdot \theta_i^2 \cdot dSRP2_i + \tau_3 \cdot \theta_i^3 \cdot dSRP3_i \quad (17)$$

where τ_3 is a step parameters of SPR_i like τ_1 and τ_2 , θ_i^3 also is generated randomly in the range $(0, 1)$. $dSRP3_i = (dSRP3_i^1, dSRP3_i^2, \dots, dSRP3_i^d, \dots, dSRP3_i^D)$ is a vector and defined as follows:

$$dSRP3_i^d = \frac{SRP_{i,\beta}^d + SRP_{i,\beta}^d + SRP_{i,\beta}^d}{3} + r_3 \cdot (SRP_{i,best}^d - SRP_i^d) + r_4 \cdot (SRP_j^d - SRP_i^d) \quad (18)$$

where r_3, r_4 and r_5 are three random vectors in $[0, 1]$, $SRP_{i,best}$ denotes the best position of i -th raindrop in the past. $SRP_{i,\beta}^d, SRP_{i,\gamma}^d$ and $SRP_{i,\delta}^d$ are define as

$$SRP_{i,\beta}^d = SRP_{i,\beta}^d - a_1 \cdot |a_2 \cdot SRP_{i,\beta}^d - SRP_i^d| \quad (19)$$

$$SRP_{i,\gamma}^d = SRP_{i,\gamma}^d - a_1 \cdot |a_2 \cdot SRP_{i,\gamma}^d - SRP_i^d| \quad (20)$$

$$SRP_{i,\delta}^d = SRP_{\delta}^d - a_1 \cdot |a_2 \cdot SRP_{\delta}^d - SRP_i^d| \quad (21)$$

where a_1 and a_2 are two random number in range (0, 1), SRP_{β} , SRP_{γ} and SRP_{δ} denote the optimal raindrop, suboptimum raindrop, third-optimum raindrop.

V. EXPERIMENTS AND ANALYSIS

To demonstrate the effectiveness and efficiency of the proposed algorithm, several experiments are conducted on NSFNET and ARPANET topologies.

A. Parameters Setting

1) *Network Parameters*: Two widely used networks are used in experiments, i.e., NSFNET topology and ARPANET topology[26]. There are $N_{vnf} = 5$ types of VNFs, and each data center can provide 2-5 types of VNFs. Each VNF-SC asks for one VNF at least and required frequency slots satisfy uniform distribution in [5, 10]. In addition, ratio of required frequency slots after the realization of homologous VNFs is satisfy uniform distribution in [0.5, 1.5]. Each fiber accommodates 1000 frequency slots, i.e., $N_F = 1000$. We use four modulation levels for the subcarriers: BPSK, QPSK, 8QAM and 16QAM. So, ML can be assigned as 1, 2, 3 and 4 for different modulation levels of BPSK, QPSK, 8QAM and 16QAM. The transmission distance of modulation levels are 9600, 4800, 2400 and 1200 Km. In proposed improved artificial raindrop algorithm (IARA), following parameters are chosen: population size $P_s = 100$, maximum iterations $G_{max} = 30,000$, $\tau_1 = \tau_2 = \tau_3 = 2$.

B. Experimental Results

We compare the proposed algorithm with other several algorithms. The one is modified by the algorithm proposed in literature [5](briefly LBA). The second is LF-LBA, which includes least fist strategy and LBA algorithm. In addition, we also compared IARA with ARA (artificial raindrop algorithm, ARA), which proposed in literature [27].

To demonstrate the performance of proposed model and algorithm, two experimental scenes are conducted. In the first scene, we fixed the number of destination nodes as $N_D = N_V/3$ and $N_D = 2N_V/3$, i.e., $N_d = N_D/N_V = 1/3$ and $N_d = N_D/N_V = 2/3$. That is to say, the number of destination nodes is generated in $[N_V/6, N_V/3]$ and $[N_V/3, 2N_V/3]$ randomly. These nodes are selected from each topology randomly. Fig.2 and Fig.3 show the experimental results in NSFNET and ARPANET topology when $\alpha = 1$. Experimental results in NSFNET and ARPANET topology when $\beta = 1$ is shown in Fig.4 and Fig.5. Fig.6 and Fig.7 show the experimental results in NSFNET and ARPANET topology when $\gamma = 1$. Experimental results in NSFNET and ARPANET topology when $\alpha = \beta = \gamma = 1/3$ is shown in Fig.8 and Fig.9. In each experiment, number of connection requests are set as $N_R = \rho N_V(N_V - 1)$, and $\rho = 0.25, 0.5, 1, 2$ and 4 , respectively.

In the second scene, we fixed the three weights α_1, α_2 and α_3 as $\alpha_1 = \alpha_2 = \alpha_3 = 1/3$. Fig.10 to Fig.14 show the results obtained in NSFNET topology and ARPANET topology when $\rho = 0.25, \rho = 0.5, \rho = 1, \rho = 2$ and $\rho = 4$, respectively. In each experiment, the number of connection requests are set as $N_D = \theta N_V$, and θ is selected as 0.2, 0.4, 0.6, 0.8 and 1, respectively.

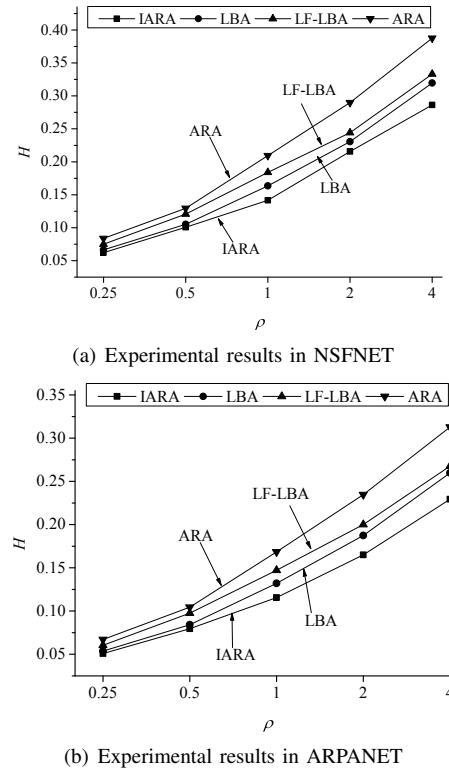


Fig. 2. Experimental results in two topologies when $\alpha = 1, N_D = N_V/3$.

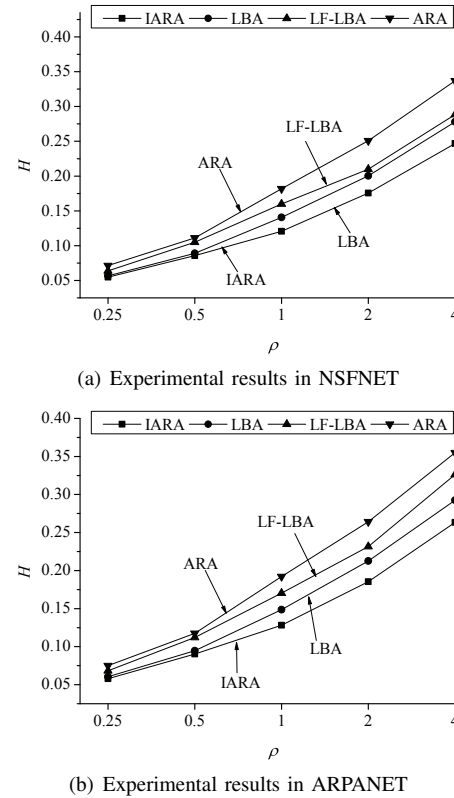
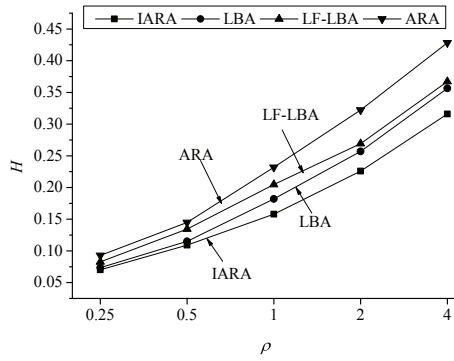
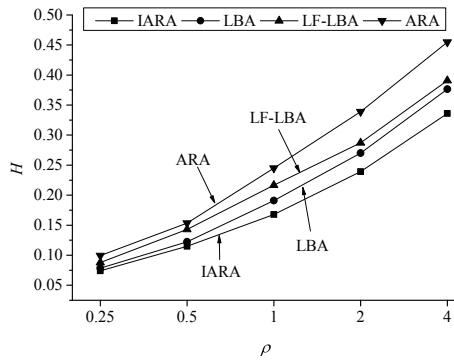


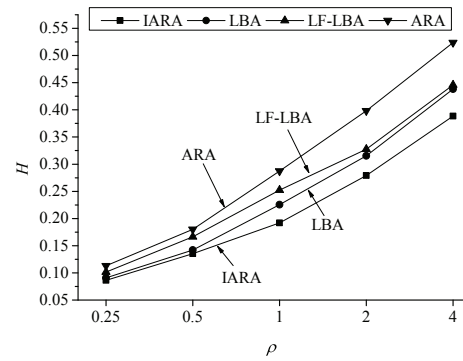
Fig. 3. Experimental results in two topologies when $\alpha = 1, N_D = 2N_V/3$.



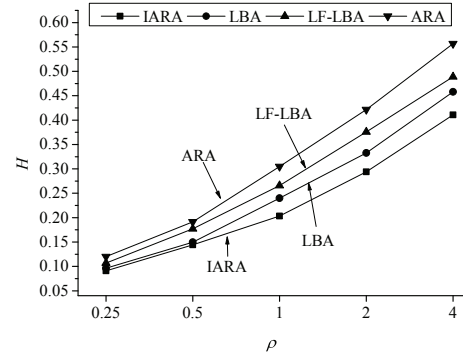
(a) Experimental results in NSFNET



(b) Experimental results in ARPANET



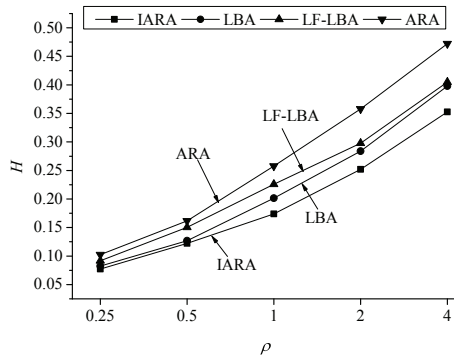
(a) Experimental results in NSFNET



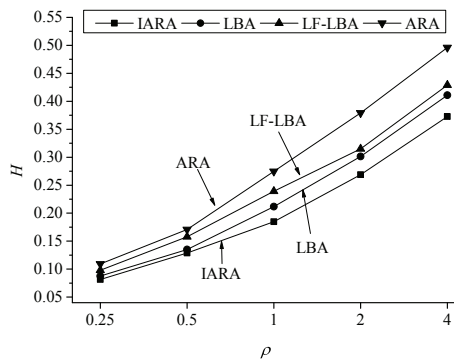
(b) Experimental results in ARPANET

Fig. 4. Experimental results in two topologies when $\beta = 1, N_D = N_V/3$.

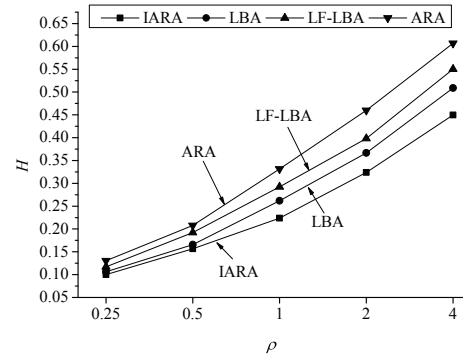
Fig. 6. Experimental results in two topologies when $\gamma = 1, N_D = N_V/3$.



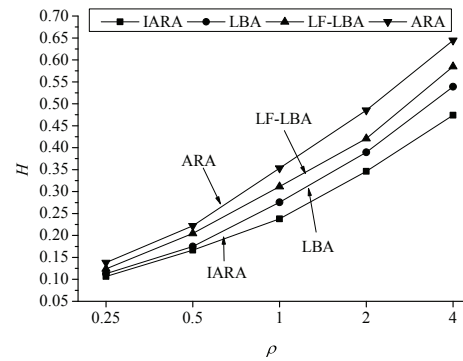
(a) Experimental results in NSFNET



(b) Experimental results in ARPANET



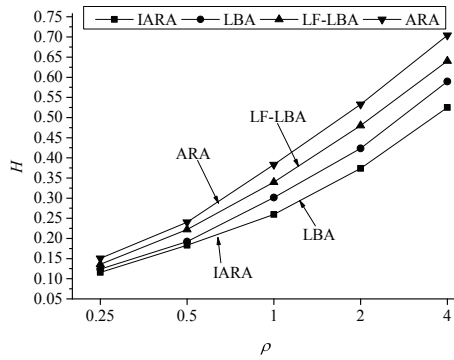
(a) Experimental results in NSFNET



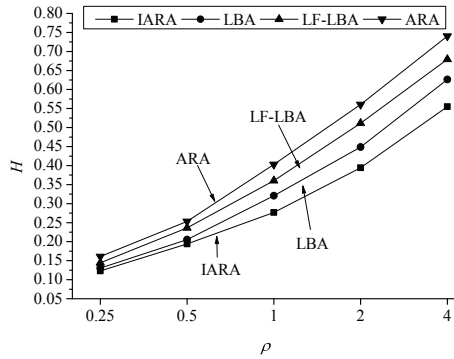
(b) Experimental results in ARPANET

Fig. 5. Experimental results in two topologies when $\beta = 1, N_D = 2N_V/3$.

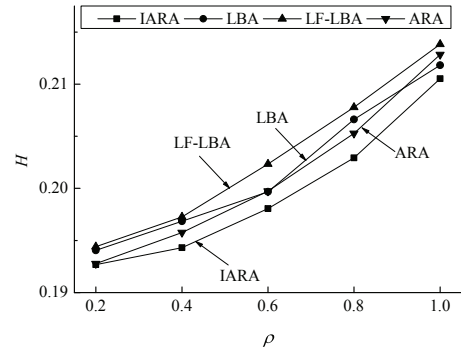
Fig. 7. Experimental results in two topologies when $\gamma = 1, N_D = 2N_V/3$.



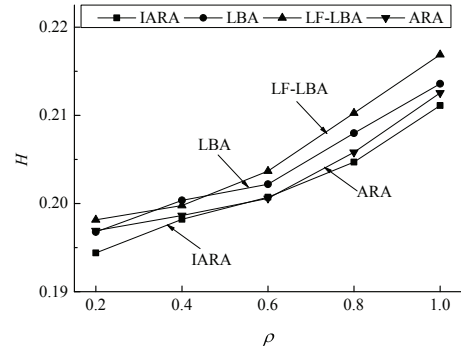
(a) Experimental results in NSFNET



(b) Experimental results in ARPANET



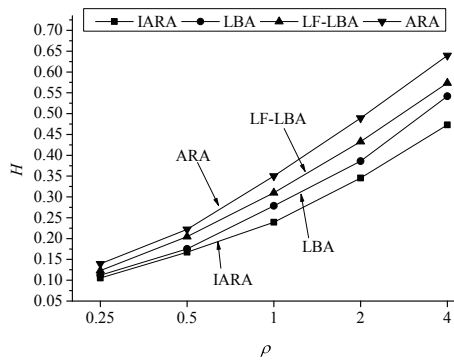
(a) Results obtained in NSFNET



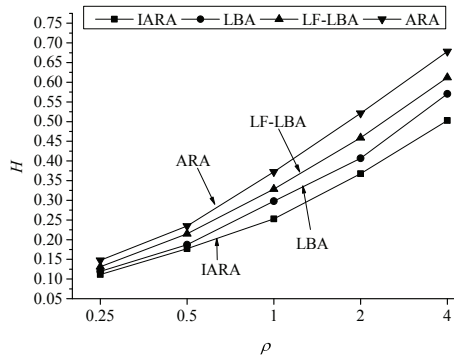
(b) Results obtained in ARPANET

Fig. 8. Experimental results in two topologies when $\alpha = \beta = \gamma = 1/3, N_D = N_V/3$.

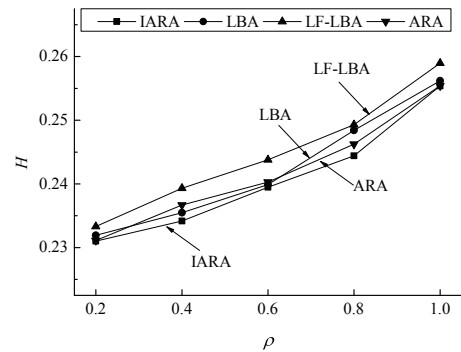
Fig. 10. Experimental results obtained when $\rho = 0.25$.



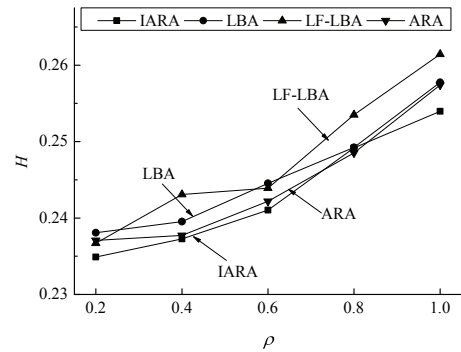
(a) Experimental results in NSFNET



(b) Experimental results in ARPANET



(a) Results obtained in NSFNET



(b) Results obtained in ARPANET

Fig. 9. Experimental results in two topologies when $\alpha = \beta = \gamma = 1/3, N_D = 2N_V/3$.

Fig. 11. Experimental results obtained when $\rho = 0.5$.

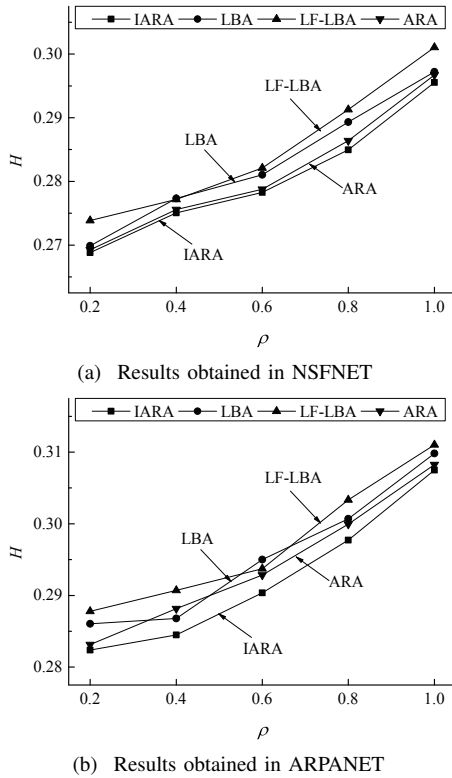


Fig. 12. Experimental results obtained when $\rho = 1$.

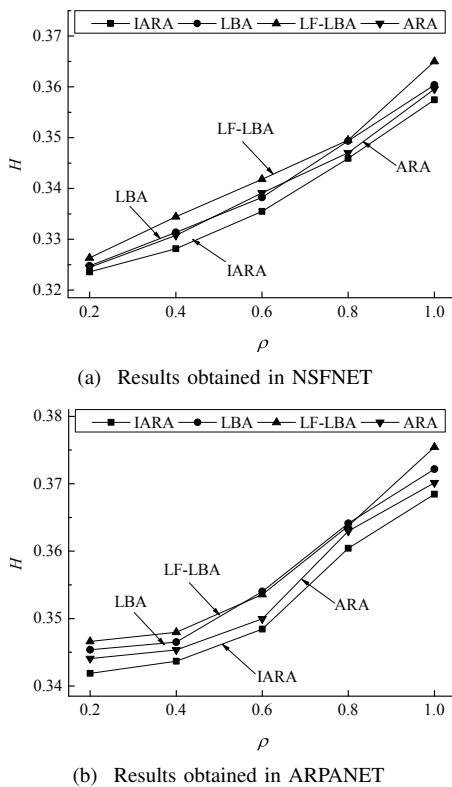


Fig. 13. Experimental results obtained when $\rho = 2$.

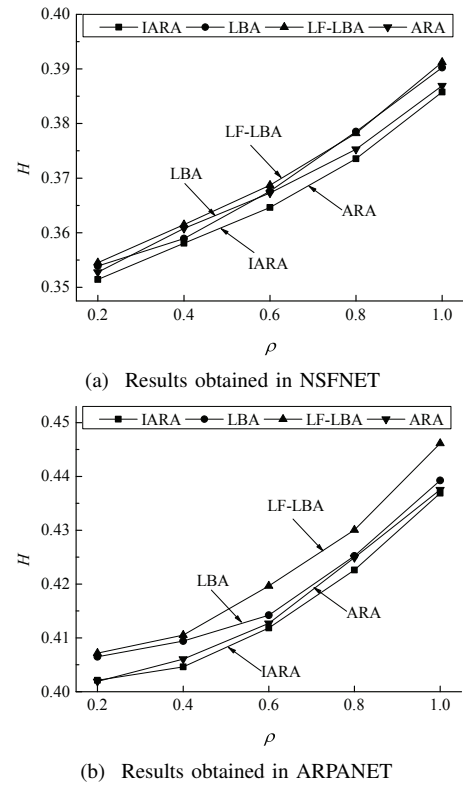


Fig. 14. Experimental results obtained when $\rho = 4$.

C. Experimental Analysis

The experimental results obtained in NSFNET and US Backbone topology are shown in Fig.2 and Fig.3 when α, β and γ are selected as 1, 0 and 0, respectively. Thus, the objective function is to minimize the maximum index of used frequency slots (MIUFS). From the experimental results, we can see that the proposed algorithm (IGWO) obtained the better results than the compared algorithms. In general, least first strategy can decrease the maximum index of used frequency slots. However, VNF dependency can make it disabled. So, LBA can obtained the better results than LF-LBA in some cases, and LF-LBA is better than LBA in other scenarios. The proposed algorithm IGWO can find optimal routing and VNFs deployment schemes for all the VNF-SC. So, IGWO can obtain the best solution among the three algorithms. The MIUFS obtained by the IGWO is 2.8%-5.2% less than those obtained by algorithms LBA and LF-LBA when the number of connection requests is $0.25N_V(N_V - 1)$. When the number of connection requests is $2N_V(N_V - 1)$, the MIUFS obtained by IGWO is 9.1%-10.9% less than those obtained by algorithms LBA and LF-LBA, respectively. That is to say, the IGWO can obtain a smaller total power consumption and save more power used than LBA and LF-LBA with the increase of the number of connection requests. From the experimental results, we also can see that the MIUFS obtained in US Backbone topology is smaller than that obtained in NSFNET topology for the same ρ . Since there are more node in US Backbone topology, it has more DC. So, the VNF-SCs can distributed in the DCs balanced. Thus, the MIUFS obtained in US Backbone topology is smaller than that obtained in NSFNET topology for the same ρ .

When α, β and γ are selected as 0, 1 and 0, the experimen-

tal results in two topologies are shown in Fig.4 and Fig.5. Similar to the experimental results in Fig.2 and Fig.3, we also can see that the proposed algorithm (IGWO) obtained the better results than the compared algorithms. In addition, we can not tell that LBA is better than LF-LBA or LF-LBA is better than LBA according to the experimental results.

Fig.6 and Fig.7 show the experimental results when α , β and γ are selected as 1, 0 and 0. Fig.8 and Fig.9 show the experimental results when $\alpha = \beta = \gamma = 1/3$. From the experimental results, we can see that proposed algorithm (IARA) can obtain the better solution than the two compared algorithms.

As shown in the experimental results, we can see IARA can obtain the better results than that obtained by ARA. In the IARA, we improved the strategy of position update method for the individual. The position of other individual and its past position information are used like PSO and DE. So it can enhance the search ability and increase the convergent speed. In addition, the parameter μ is used. It can help to take advantage of the trajectory information of the individuals. When $\mu = 1$, the proposed IARA degraded to the standard ARA algorithm. Position update method can use the past μ position information when $\mu \geq 1$. Thus, IARA is better than ARA for this optimization problem. That is to say, IARA can obtain the better solution than ARA.

VI. CONCLUSION

We studied the problem of VNFs deployment for VNF-SC in inter-data center elastic optical networks. In inter-data center elastic optical networks, each data center only can provide some specific VNFs, and system resource is limited. We establish a mix-integer linear programming model and propose an improved artificial raindrop algorithm (IARA) algorithm to solve the model. Simulation experiments are conducted on two network topologies, and experimental results show that the proposed algorithm can obtain a better solution than compared algorithms.

REFERENCES

- [1] R. Mijumbi, J. Serrat, J.-L. Gorricho, N. Bouten, F. D. Turck, and R. Boutaba, "Network function virtualization: State-of-the-art and research challenges," *IEEE Communications Surveys Tutorials*, vol. 18, no. 1, pp. 236–262, 2016.
- [2] J. Pei, P. Hong, M. Pan, J. Liu, and J. Zhou, "Optimal VNF placement via deep reinforcement learning in SDN/VNF-enabled networks," *IEEE Journal on Selected Areas in Communications*, vol. 38, no. 2, pp. 263–278, 2020.
- [3] Z. Ye, X. Cao, J. Wang, H. Yu, and C. Qiao, "Joint topology design and mapping of service function chains for efficient, scalable, and reliable network functions virtualization," *IEEE Network*, vol. 30, no. 3, pp. 81–87, 2016.
- [4] L. Xu, A. Deng, M. Ge, J. Shi, and G. Gao, "A MADM-based handover management in software-defined 5G network," *Engineering Letters*, vol. 27, no. 4, pp. 842–849, 2019.
- [5] W. Fang, M. Zeng, X. Liu, W. Lu, and Z. Zhu, "Joint spectrum and IT resource allocation for efficient vNF service chaining in inter-datacenter elastic optical networks," *IEEE Communications Letters*, vol. 20, no. 8, pp. 1539–1542, 2016.
- [6] H. Tang, D. Zhou, and D. Chen, "Dynamic network function instance scaling based on traffic forecasting and VNF placement in operator data centers," *IEEE Transactions on Parallel and Distributed Systems*, vol. 30, no. 3, pp. 530–543, 2019.
- [7] M. Xia, M. Shirazipour, Y. Zhang, H. Green, and A. Takacs, "Network function placement for NFV chaining in packet/optical datacenters," *Journal of Lightwave Technology*, vol. 33, no. 8, pp. 1565–1570, 2015.
- [8] H. Xuan, Y. Wang, Z. Xu, S. Hao, and X. Wang, "New optimization model for routing and spectrum assignment with nodes insecurity," *Optics Communications*, vol. 389, pp. 42–50, 2017.
- [9] H. Zhang, G. Wu, and W. Bu, "Research of agent based control model for embedded networked system," *Engineering Letters*, vol. 27, no. 2, pp. 278–286, 2019.
- [10] M. Zeng, J. Fang, and Z. Zhu, "Orchestrating tree-type VNF forwarding graphs in inter-DC elastic optical networks," *Journal of Lightwave Technology*, vol. 34, no. 14, pp. 3330–3341, 2016.
- [11] S. Li, K. Yuan, Y. Zhang, and W. Sun, "A novel bandwidth allocation scheme for elastic and inelastic services in peer-to-peer networks," *IAENG International Journal of Computer Science*, vol. 46, no. 2, pp. 163–169, 2019.
- [12] H. Xuan, S. Wei, X. Zhao, Y. Zhou, X. Ma, D. Liu, and Y. Li, "Unavailable time aware scheduling of hybrid task on heterogeneous distributed system," *IAENG International Journal of Applied Mathematics*, vol. 50, no. 1, pp. 133–146, 2020.
- [13] M. Dieye, S. Ahvar, J. Sahoo, E. Ahvar, R. Glitho, H. Elbiaze, and N. Crespi, "CPVNF: Cost-efficient proactive VNF placement and chaining for value-added services in content delivery networks," *IEEE Transactions on Network & Service Management*, vol. 15, no. 2, pp. 774–786, 2018.
- [14] E. Vincenzo, M. Emanuele, and A. Mostafa, "An approach for service function chain routing and virtual function network instance migration in network function virtualization architectures," *IEEE/ACM Transactions on Networking*, vol. 25, no. 4, pp. 2008–2025, 2017.
- [15] J. G. Herrera and J. F. Botero, "Resource allocation in VNF: A comprehensive survey," *IEEE/ACM Transactions on Networking*, vol. 13, no. 3, pp. 518–532, 2016.
- [16] L. Wang, Z. Lu, X. Wen, R. Knopp, and R. Gupta, "Joint optimization of service function chaining and resource allocation in network function virtualization," *IEEE Access*, vol. 4, no. 1, pp. 8084–8094, 2017.
- [17] M. Till Beck and J. Felipe Botero, "Scalable and coordinated allocation of service function chains," *Computer Communications*, vol. 102, no. 1, pp. 78–88, 2017.
- [18] A. Razzaq, A. M.Khedr, and Z. Al Aghbari, "Distributed fault tolerant target tracking protocol for new face-based wireless sensor networks," *IAENG International Journal of Computer Science*, vol. 47, no. 2, pp. 250–261, 2020.
- [19] T. Gao, X. Li, Y. Wu, W. Zou, and B. Mukherjee, "Cost-efficient VNF placement and scheduling in public cloud networks," *IEEE Transactions on Communications*, vol. 68, no. 8, pp. 4946–4959, 2020.
- [20] M. Mechtri, C. Ghribi, and D. Zeghlache, "A scalable algorithm for the placement of service function chains," *IEEE Transactions on Network and Service Management*, vol. 13, no. 3, pp. 533–546, 2016.
- [21] X. Chen, Z. Zhu, J. Guo, S. Kang, R. Proietti, A. Castro, and S. Yoo, "Leveraging mixed-strategy gaming to realize incentive-driven VNF service chain provisioning in broker-based elastic optical inter-datacenter networks," *IEEE/OSA Journal of Optical Communications and Networking*, vol. 10, no. 2, pp. A232–A240, 2018.
- [22] B. Li, W. Lu, S. Liu, and Z. Zhu, "Deep-learning-assisted network orchestration for on-demand and cost-effective vNF service chaining in inter-DC elastic optical networks," *IEEE/OSA Journal of Optical Communications and Networking*, vol. 10, no. 10, pp. D29–D41, 2018.
- [23] P. T. A. Quang, A. Bradai, K. D. Singh, G. Picard, and R. Riggio, "Single and multi-domain adaptive allocation algorithms for VNF forwarding graph embedding," *IEEE Transactions on Network and Service Management*, vol. 16, no. 1, pp. 98–112, 2018.
- [24] X. Chen, Z. Zhu, R. Proietti, and S. B. Yoo, "On incentive-driven vNF service chaining in inter-datacenter elastic optical networks: a hierarchical game-theoretic mechanism," *IEEE Transactions on Network and Service Management*, vol. 16, no. 1, pp. 1–12, 2018.
- [25] M. Tajiki, S. Salsano, L. Chiaraviglio, M. Shojafar, and B. Akbari, "Joint energy efficient and QoS-aware path allocation and VNF placement for service function chaining," *IEEE Transactions on Network and Service Management*, vol. 16, no. 1, pp. 374–388, 2018.
- [26] S. J. Savory, "Congestion aware routing in nonlinear elastic optical networks," *IEEE Photonics Technology Letter*, vol. 26, no. 10, pp. 1057–1060, 2014.
- [27] Q. Jiang, L. Wang, Y. Lin, X. Hei, and X. Lu, "An efficient multi-objective artificial raindrop algorithm and its application to dynamic optimization problems in chemical processes," *Applied Soft Computing*, vol. 58, no. 5, pp. 354–377, 2017.